Nuclear Activity in Galaxies Across Cosmic Time
Proceedings IAU Symposium No. 356, 2019
M. Pović, P. Marziani, J. Masegosa, H. Netzer, S. H. Negu & S. B. Tessema, eds.
doi:10.1017/S1743921320002586

A new tool to derive chemical abundances in type-2 active galactic nuclei

Rubén García-Benito[1], Enrique Pérez-Montero[1], Oli L. Dors[2], José M. Vílchez[1], Monica V. Cardaci[3,4] and Guillermo F. Hägele[3,4]

[1]Instituto de Astrofísica de Andalucía, Apartado de correos 3004, E-18080 Granada, Spain
emails: rgb@iaa.es, epm@iaa.es

[2]Universidade do Vale do Paraíba, Av. Shishima Hifumi, 2911, Cep 12244-000, São José dos Campos, SP, Brazil

[3]Instituto de Astrofísica de La Plata (CONICET-UNLP), Argentina

[4]Facultad de Ciencias Astronómicas y Geofísicas, Universidad Nacional de La Plata, Paseo del Bosque s/n, 1900 La Plata, Argentina

Abstract. We present a new tool for the analysis of the optical emission lines of the gas in the Narrow Line Region (NLR) around Active Galactic Nuclei (AGNs). This new tool can be used in large samples of objects in a consistent way using different sets of optical emission-lines taking into the account possible variations from the O/H - N/O relation. The code compares certain observed emission-line ratios with the predictions from a large grid of photoionization models calculated under the most usual conditions in the NLR of AGNs to calculate the total oxygen abundance, nitrogen-to-oxygen ratio and ionization parameter. We applied our method to a sample of Seyfert 2 galaxies with optical emission-line fluxes from the literature. Our results confirm the high metallicity of the objects of the sample and provide consistent values with the direct method. The usage of models to calculate precise ICFs is mandatory when only optical emission lines are available to derive chemical abundances using the direct method in NLRs of AGN.

Keywords. methods: data analysis, ISM: abundances, galaxies: abundances, galaxies: active, galaxies: Seyfert

1. Introduction

The energetic radiation coming from the central black holes in galaxies is partially re-emitted by the surrounding gas as very bright emission lines which in turn can be used to derived the physical conditions in these extreme regions. Since they can be observed up to very high redshifts, Active galactic Nuclei (AGNs) are thus a powerful source for the study of cosmic evolution of galaxies.

It is widely accepted (Ferland & Netzer 1983) that the main mechanism of the narrow-line region (NLR) in AGNs is photoionization. However, it is also known that the total metallicity derived using the direct method (i.e. the T_e method) gives sub-solar metallicities in AGNs, as compared to the predictions from photoionization models. Using a sample of NLRs of AGNs, Dors *et al.* (2015) found that the T_e-method using the optical lines underestimated the oxygen abundances by an averaged value of ∼0.8 dex as compared to calibrations based on photoionization models.

Models are, therefore, a powerful tool to interpret the observed lines and provide valuable information to study chemical abundances. In this work, we describe a new code based on photoionization models to derive chemical abundances in the NLR in AGNs.

2. The code

In Pérez-Montero *et al.* (2019) we present a full description of a new code to derive the total oxygen abundance, nitrogen-to-oxygen ratio (N/O), and the ionization parameter (U) from the analysis of optical emission lines in the NLR of type-2 AGNs. The code is based on the well proven HII-CHI-MISTRY† code (hereafter HCM, Pérez-Montero 2014) originally developed for the analysis of star-forming regions. The advantages of the code are: a) it can be applied to a large number of objects in an automatic way; b) all objects are analyzed in a consistent way regardless of the set of input emission lines; c) it provides uncertainties for all the estimated quantities; d) it provides an independent estimation of the N/O ratio; and e) it is consistent with the direct method.

The code uses a grid of 5 865 photoionization models run with the code Ferland *et al.* (2017) v.17.01. The models cover a wide range of the parameters space with typical NLRs conditions (see Pérez-Montero *et al.* 2019 for further details). The spectral energy distribution (SED) is composed by two components: the Big Blue Bump at 1 Ryd and a power law with spectral index $\alpha_X = -1$. The continuum between 2KeV and 2500 Å is modeled by a power law with spectral index $\alpha_{OX} = -0.8$. All models were calculated using a spherical geometry with a filling factor of 0.1, a standard dust-to-gas ratio and a constant density of 500 particles per cm^{-3}. In addition we checked the effect of changing in the models the α(ox) down to -1.2 and enhancing the electron density up to 2 000 cm^{-3} but no noticeable changes were found in the calculation of the chemical abundances using the method described here. For more details on the results of these comparison see Pérez-Montero *et al.* (2019). The models cover the range of 12 + log(O/H) from 6.9 to 9.1 in bins of 0.1 dex. The N/O range goes from -2.0 to 0.0 in bins of 0.125 dex and log U from -4.0 to -0.5 in bins of 0.25 dex.

The code uses as input the reddening-corrected relative-to-Hβ emission line intensities from [[O II]] λ3727 Å, [Ne III] λ3868 Å, [[O III]] λ4363 Å, [[O III]] λ5007 Å, [[N II]] λ6583 Å, and [S II] $\lambda\lambda$6717+6731 Å with their corresponding errors. However, the code is adapted to provide also a solution in case one or several of these lines are not given.

In short, the work-flow of the code is as follows. First, the code constrain the parameter space searching for N/O as a weighted mean over all models, using optical emission lines for similar excitation, such as the ratio [[N II]]λ6583/[[O II]]λ3727 or [[N II]]λ6583/[S II]$\lambda\lambda$6717+6731. These ratios do not show almost any dependence on excitation and therefore N/O can be calculated without any assumption about the ionization parameter. Using the uncertainties of all the input observed lines, the code calculates the error using a Monte Carlo simulation. A set of line ratios such as [[O III]]λ5007/[[O III]]λ4363, [[N II]]λ6583/Hα,

$$\mathrm{R23} = \frac{[\mathrm{OII}]\lambda3727 + [\mathrm{OIII}]\lambda\lambda4959 + 5007}{\mathrm{H}\beta},$$

$$\mathrm{O3N2} = \log\left(\frac{[\mathrm{OIII}]\lambda5007}{\mathrm{H}\beta} \cdot \frac{\mathrm{H}\alpha}{[\mathrm{NII}]\lambda6583}\right),$$

or

$$\mathrm{O2Ne3} = \frac{[\mathrm{OII}]\lambda3727 + [\mathrm{NeIII}]\lambda3868}{\mathrm{H}\beta}$$

(depending on the availability of the observed lines) are used in a second iteration to sample a subset of models constrained to the N/O values previously calculated to obtain the oxygen abundance and the ionization parameter.

† Publicly available in the webpage https://www.iaa.csic.es/ epm/HII-CHI-mistry.html.

https://doi.org/10.1017/S1743921320002586 Published online by Cambridge University Press

Table 1. Mean and standard deviation of the residuals between the O/H from Dors *et al.* (2017) and the values derived by HCM using different input lines as shown in Figure 1. In the table [[O II]] stands for λ3727 Å, $[[O\,III]]_n$ for λ5007 Å, [[N II]] for λ6583 Å, and [S II] for $\lambda\lambda$6717+6731 ÅÅ.

Input emission lines	Mean Δ(O/H)	St.dev. Δ(O/H)
All lines	−0.01	0.21
$[[O\,III]]_n$, [[N II]], [S II]	+0.15	0.26
[[O II]], $[[O\,III]]_n$	−0.11	0.21
$[[O\,III]]_n$, [[N II]]	−0.24	0.15
[[N II]]	−0.25	0.16
[[N II]], [S II]	+0.29	0.29

3. Results

3.1. *The control sample*

No empirical derivation of chemical abundances (i.e. no abundances using the direct method) in the NLR of AGNs using optical emission lines are available in the literature. Therefore, we use as a control sample the abundance estimations by Dors *et al.* (2017) obtained from detailed tailored photoionization models using the CLOUDY code. They compiled a sample of 47 Seyfert 1.9 and 2 galaxies at a redshift $z \leqslant 0.1$ providing the most prominent optical emission lines, including the auroral line [OIII] 4363 Å. They do not provide an error estimation of the oxygen abundances obtained from their models.

3.2. *Comparisons*

In Fig. 1 we compare the total oxygen abundance derived for the control sample by Dors *et al.* (2017) with those obtained by HCM when all or only some of the input lines are used†. The option of restricting the number of input lines simulates common observing conditions when only limited sensitivity or spectral coverage of the detector is available. The left upper panel shows the best case scenario when all possible emission lines are provided. There is a good agreement between both sets with a dispersion of 0.21 dex and a residual of -0.01 dex. The upper right panel displays the relation when lines [[O III]] λ 4363 Å and [[O II]] λ 3727 Å are not included. This is common case when the blue part of the spectrum is not available (e.g. in the Sloan Digital Sky Survey at very low redshifts) and the [[O III]] λ 4363 Å is to faint to be observed. In this case, the dispersion is nearly the same but the residual increases by 0.1 dex. Even when only a couple of lines or only [NII] λ 6583 Å is available the agreement is good, with deviations from the abundances lower than the usual uncertainties. Table 1 shows the mean and standard deviation of the residuals of the comparison cases presented in Fig. 1.

3.3. *Consistency with the direct method*

There is known discrepancy between the chemical abundances derived using the T_e method in NLRs of type-2 AGNs, leading to very low values if compared to those obtained from some photoionization models (e.g. Dors *et al.* 2015). The code HCM has proved to be in accordance with the T_e method in star-forming regions (Pérez-Montero 2014). Thus, we can use HCM to investigate the possible origin of the discrepancies in AGNs.

In Fig. 2 we show the total oxygen abundance derived by Dors *et al.* (2017) for their sample of Sy2 galaxies, compared to the addition of the abundances of the most prominent

† More detailed comparisons including N/O and the ionization parameter can be found in Pérez-Montero *et al.* (2019).

https://doi.org/10.1017/S1743921320002586 Published online by Cambridge University Press

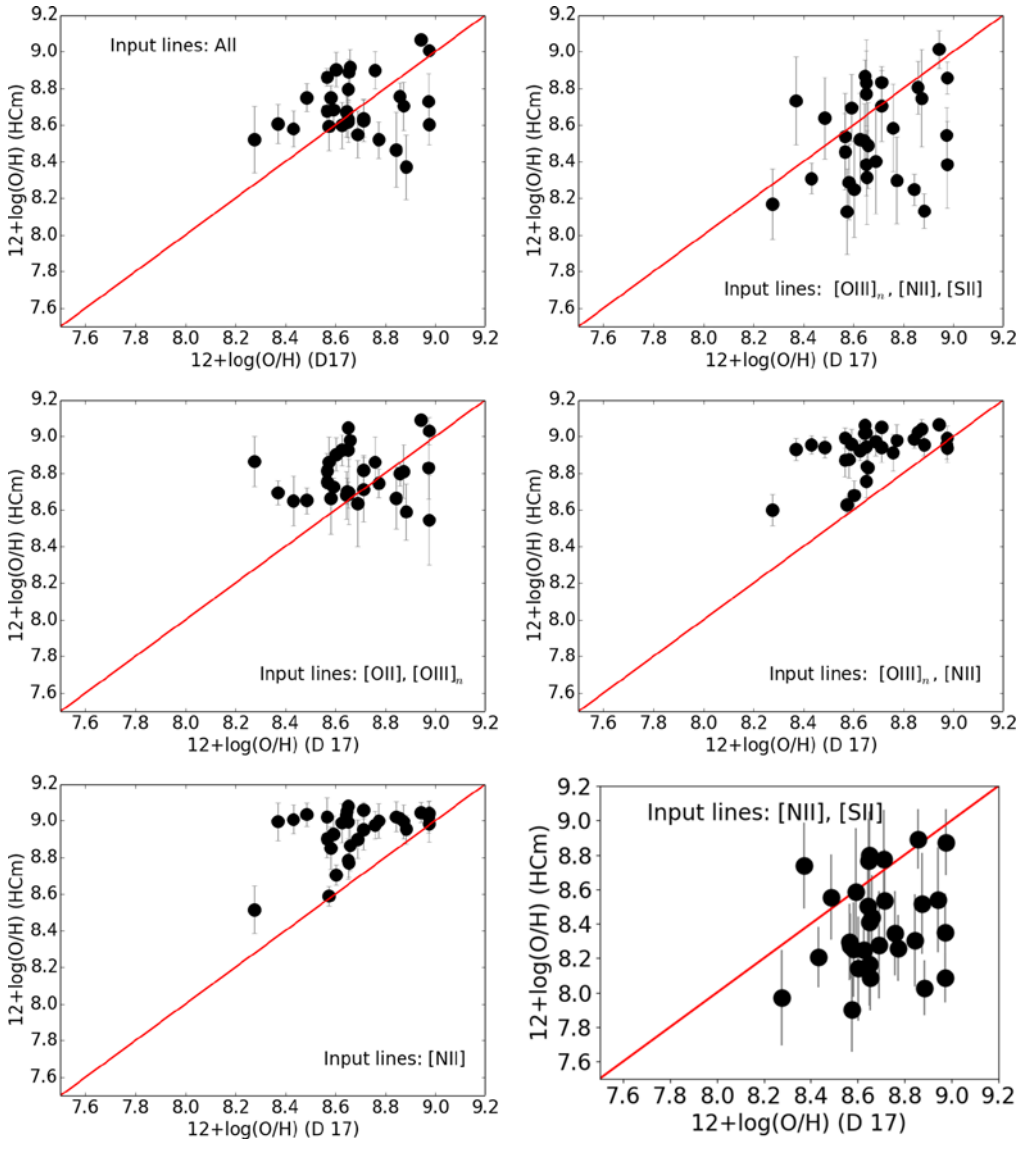

Figure 1. Comparison between total oxygen abundances 12 + log(O/H) derived using the method described in this work (HCM) and those taken from Dors *et al.* (2017) from tailored photoionization models. *Upper left*: comparison when all the lines are used. *Upper right*: comparison in the absence of [[O III]] λ 4363 Å and [[O II]] λ 3727 Å. *Middle left*: comparison when only [[O II]] λ 3727 Å and [[O III]] λ 5007 Å are included. *Middle right*: comparison when only [[O III]] λ 5007 Å and [[N II]] λ 6583 Å are included. *Bottom left*: comparison when only [[N II]] λ 6583 Å is provided. *Bottom right*: comparison when only [[N II]] λ 6583 Å and [S II] λ 6717+6731 ÅÅ are included. The solid line represents the 1:1 relation. In the legend [[O II]] stands for λ3727 Å, [[O III]]$_n$ for λ5007 Å, [[N II]] for λ6583 Å, and [S II] for $\lambda\lambda$6717+6731 ÅÅ.

oxygen ionic species in the optical part of the spectrum, i.e. O^+ and O^{2+}, calculated using the T_e method. The addition of the relative ionic abundances of the oxygen is 0.7 dex lower that the one derived by the models. Figure 2 shows also predictions from the grid of models for different ionization parameter values. The difference is well explained as an important dependence on the total metallicity and ionization parameter. This result

https://doi.org/10.1017/S1743921320002586 Published online by Cambridge University Press

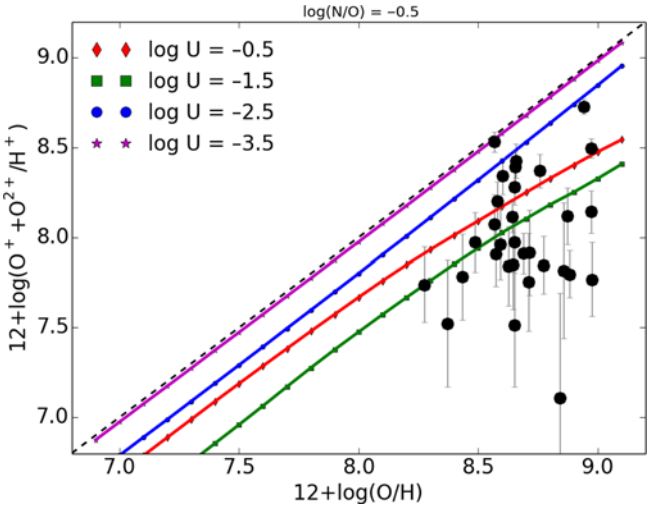

Figure 2. Comparison between total oxygen abundance and the addition of the abundances of the two main oxygen ions O^+ and O^{2+} observed in the optical part of the spectrum. Models are represented using solid lines for different values of U. Black circles represent the data from Dors *et al.* (2017) whose total abundances where calculated using tailored models, while their ionic abundances were calculated following the T_e method. The dashed black line represents the 1:1 relation.

highlights the importance of using models to derive the total oxygen abundance in NLRs of AGNs when only opital lines are available, as ionization correction factors (ICFs) are far to be negligible, contrary to star-forming regions.

References

Dors, O. L., Cardaci, M. V., Hägele, G. F., Rodrigues, I., Grebel, E. K., Pilyugin, L. S., Freitas-Lemes, P., Krabbe, A. C., *et al.* 2015, *MNRAS* 453, 4102

Dors, Jr. O. L., Arellano-Córdova, K. Z., Cardaci, M. V., Hägele, G. F., *et al.* 2017, *MNRAS*, 468, L113

Ferland, G. J. & Netzer, H. 1983, *ApJ*, 264, 105

Ferland *et al.* 2017, *Rev. Mexicana AyA* 53, 385

Pérez-Montero, E. 2014, *MNRAS* 441, 2663

Pérez-Montero, E., Dors, O. L., Vílchez, J. M., García-Benito, R., Cardaci, M. V., Hägele, G. F., *et al.* 2019, *MNRAS*, 489, 2652

https://doi.org/10.1017/S1743921320002586 Published online by Cambridge University Press